

Facile synthesis of chitosan/CuO nanocomposites for potential use as biocontrol agents

P. SIRIPHANNON^{1,2*} and Y. IAMPHAOJEEN²

¹Department of Chemistry, Faculty of Science, King Mongkut's Institute of Technology Ladkrabang,
Chalongkrung Road, Ladkrabang, Bangkok 10520, Thailand

²Functional Nanostructured Materials Laboratory, College of Nanotechnology, King Mongkut's Institute of Technology Ladkrabang,
Chalongkrung Road, Ladkrabang, Bangkok 10520, Thailand

Abstract. Chitosan/CuO nanocomposites (Chi/CuO) were prepared by facile and eco-friendly technique. The 2%w/v chitosan solution was mixed with 0.5 %w/w sodium tripolyphosphate (STPP), resulting in the formation of ionically crosslinked chitosan. The crosslinked chitosan was soaked in an aqueous solution containing 0.001, 0.01 or 0.1 mol/L $\text{CuSO}_4 \cdot 5\text{H}_2\text{O}$ for 24 hrs, in which the Cu^{2+} ions were absorbed into the chitosan network, forming as the chitosan/ Cu^{2+} precursors. The chitosan/ Cu^{2+} precursors were hydrothermally reacted in two different basic media, i.e. NaOH and NH_4OH , at 100°C for 24 hrs, resulting in the nano-sized CuO crystals hydrothermally grew and embedded in the crosslinked chitosan matrix. The CuO grown in the NaOH possessed larger crystallite size and higher crystallinity than that in the NH_4OH . In addition, the CuO crystallite size in the nanocomposites increased with the increase of initial concentration of Cu^{2+} starting agent due to the increase of Cu^{2+} quantity in the chitosan/ Cu^{2+} precursors. The chitosan/CuO nanocomposites prepared by using 0.01 and 0.1 mol/L Cu^{2+} could exhibit the antibacterial activities after intimate contact with *Staphylococcus aureus* and *Escherichia coli* under JIS L 1902:1998 (Qualitative) test method, indicating their potential use as biocontrol agents.

Key words: chitosan, CuO, nanocomposite, hydrothermal, antibacterial activity.

1. Introduction

Copper oxide (CuO) is one of the most common members of copper compounds, which possesses many useful properties, e.g. semiconductivity, superconductivity, photocatalytic activity, antimicrobial activity, etc., therefore, it has been applied for diverse applications [1–5]. Among various merit properties, the antimicrobial activity of CuO has attracted the attention of many researchers because it is safe, easily released from human body, relatively stable and cheaper than silver which is the most popular antimicrobial agent [6]. In addition, the CuO nanoparticles of small size and large surface area have been reported efficient in fighting a wide range of bacterial pathogens, including the nosocomial infections caused by bacteria [4].

Various methods have been studied and developed for synthesis of CuO nanoparticles, such as mechanochemical method [7], sol-gel method [8], microwave irradiation [9–10], reverse micelle [11], hydrothermal reaction [12–13], etc., in which they tailored different particle size, morphology and crystallinity of the CuO product. In the present work, we aimed to create the CuO nanoparticles by using a three-dimensional network structure of biopolymer as a template material for nucleation and growth of CuO, i.e. crosslinked chitosan. The chitosan was selected because it is low cost, natural, biocompatible polymer with antimicrobial activity; therefore, it has been

commonly used in medical, pharmaceutical and agricultural applications [14–16]. In this study, the crosslinked chitosan acted primarily as the adsorbent material for uptake the copper (II) starting ions into its free volume cavity and then acted as the hydrothermal reactor for generating the CuO crystals. The growth of CuO crystals in the crosslinked network was considered to be constrained due to the limitation of free volume cavity, resulting in the nano-sized CuO embedded in the chitosan matrix. The effects of initial copper (II) starting ions and hydrothermal media on the growth of CuO nanoparticles in the crosslinked chitosan were investigated. The proposed technique was considered to be an eco-friendly technique for preparation of CuO nanocomposites because it could perform in mild condition using low temperature and pressure without any special equipment.

2. Experiment

2.1. Materials. Low molecular weight chitosan with a deacetylation degree (DD) of ca. 82.5% was purchased from ELAND Co.Ltd. An ionic crosslinking agent, i.e. sodium tripolyphosphate (STPP, technical grade), was purchased from UNION CHEMICAL 1986 Co.Ltd. $\text{CuSO}_4 \cdot 5\text{H}_2\text{O}$ (98%, Carlo Erba) was used as copper (II) doping agent for creating the CuO nanocrystals. NaOH (97%, Carlo Erba) and NH_4OH (30%, Carlo Erba) were used as basic reagents for hydrothermal treatments.

2.2. Preparation of crosslinked chitosan particles. The chitosan solution was prepared by dissolving 2 g of low molecular

*e-mail: punnama.si@kmitl.ac.th

Manuscript submitted 2017-06-18, revised 2017-08-27, initially accepted for publication 2017-09-27, published in June 2018.

weight chitosan in 100 ml of 2 %v/v acetic acid. The chitosan solution was then slowly added into the 0.5 %w/w sodium tripolyphosphate (STPP) aqueous solution with slow agitating in order to generate the crosslinked chitosan particles. The crosslinked chitosan particles were washed several times with deionized water and dried at ambient conditions. The crosslinked chitosan particles were analyzed by differential scanning calorimeter (DSC, Perkin Elmer, Pyris Diamond DSC) in aluminum pans over a temperature range of 50 to 400°C under nitrogen atmosphere with a constant heating rate of 10°C/min.

2.3. Preparation of chitosan/CuO nanocomposites. The crosslinked chitosan particles were soaked in an aqueous solution containing 0.001, 0.01 or 0.1 mol/L $\text{CuSO}_4 \cdot 5\text{H}_2\text{O}$ for 24 hrs, in which the Cu^{2+} ions were absorbed into the chitosan network, resulting in the chitosan/ Cu^{2+} precursors. The chitosan/ Cu^{2+} precursors were then hydrothermally reacted using two different basic solutions, i.e. NaOH and NH_4OH , in sealed glass bottles in order to grow CuO nanocrystals in the crosslinked chitosan template. The concentration of basic solution was 0.5 mol/L and the hydrothermal reaction was performed at 100°C for 24 hrs. The chitosan/CuO nanocomposites were taken out from the basic solution, rinsed several times with deionized water in a sonication bath and then dried at ambient conditions.

2.4. Characterization of chitosan/CuO nanocomposites. The quantity of adsorbed Cu^{2+} in the chitosan/ Cu^{2+} precursors was determined by X-ray fluorescence spectrometer (XRF; Bruker AG, SRS3400) using external standard addition method. An equal amount of ZnO external standard was added and homogeneously mixed with the chitosan/ Cu^{2+} precursors prior to XRF measurement, in which the relative amount of CuO/ZnO was evaluated.

The chitosan/CuO nanocomposites were characterized by X-ray diffractometer (XRD; D8 Advance, Bruker AG) and scanning electron microscope (SEM, LEO, LEO1455VP). The XRD analysis was performed using $\text{CuK}\alpha$ radiation ($\lambda = 1.54 \text{ \AA}$) with step size of 0.04°/step, scanning speed of 1°/sec and scanning range (2θ) of 20°–75°. Full width at half-maximum (FWHM) of the crystalline peak at $2\theta = 36.63^\circ$ was used to determine the crystallite size of CuO in the nanocomposites using Scherrer's equation as shown in equation (1):

$$\tau = k\lambda/\beta\cos\theta \quad (1)$$

where τ is the crystallite size (\AA), k is the shape constant (~ 0.9), λ is the wavelength (\AA), θ is the Bragg's angle (degree) and β is the observed FWHM of peak at $2\theta = 36.63^\circ$ (Radian).

2.5. Antibacterial activity test. Antibacterial activities of the chitosan/CuO nanocomposites were carried out by a simple method for primary screening. The nutrient agar plates that had been inoculated with the test organisms, i.e. *Staphylococcus aureus* (*S. aureus*) and *Escherichia coli* (*E. coli*), were prepared. The pellets of chitosan/CuO nanocomposites were gently pressed on the agar surface. The antimicrobial activities were measured by the determination of the size of the inhibition zone

after 24 hrs of incubation at $37 \pm 2^\circ\text{C}$. This test was performed according to the JIS L 1902: 1998 (Qualitative) technique.

3. Results and discussion

3.1. Characterization of crosslinked chitosan and chitosan/ Cu^{2+} precursors. Thermal behavior of the STPP ionically crosslinked chitosan was analyzed by DSC in comparison with the starting chitosan. It was found that the exothermic peaks at ca. 177°C, corresponded to the degradation of chitosan, were observed in both DSC thermograms of the starting and ionically crosslinked chitosan. However, the ionically crosslinked chitosan exhibited higher heat enthalpy (ΔH 433.8 J/g) than the starting chitosan (ΔH 197.3 J/g), insisting the formation of network structure in the ionically crosslinked chitosan.

The initial concentration of $\text{CuSO}_4 \cdot 5\text{H}_2\text{O}$ solution used in the preparation of chitosan/ Cu^{2+} precursors was varied in order to create the nanocomposites with varying amount of Cu^{2+} . The amount of Cu^{2+} adsorbed in the crosslinked chitosan was analyzed by XRF technique in comparison to the fixed amount of added ZnO external standard because the chemical compositions of chitosan matrix could not be detected by the XRF. The molar ratio of CuO/ZnO was calculated from the XRF data shown in Table 1 in order to determine the relative amount of adsorbed Cu^{2+} in the precursors. The higher initial concentration of $\text{CuSO}_4 \cdot 5\text{H}_2\text{O}$ used in the soaking system, the higher amount of CuO was detected in the precursors, indicating the higher adsorbed Cu^{2+} in the precursors.

Table 1
Chemical composition of chitosan/ Cu^{2+} precursors analyzed by XRF (ZnO was added as external standard)

Sample	Initial concentration of $\text{CuSO}_4 \cdot 5\text{H}_2\text{O}$ (mol/L)	Chemical composition (wt%)			Molar ratio of CuO/ZnO
		CuO	ZnO	Others	
Chi/0.001 Cu^{2+}	0.001	5.78	49.34	44.88	0.12
Chi/0.01 Cu^{2+}	0.01	12.12	44.53	43.35	0.28
Chi/0.1 Cu^{2+}	0.1	25.51	40.82	33.69	0.64

Figure 1 shows the relationship between initial concentration of Cu^{2+} and the molar ratio of CuO/ZnO in the precursors. It can be seen that the CuO/ZnO molar ratio steeply increased when the Cu^{2+} initial concentration was increased from 0.001 to 0.01 mol/L, however, the increase of CuO/ZnO molar ratio gradually lowered when the Cu^{2+} concentration was increased to 0.1 mol/L. This nonlinear increase of CuO/ZnO molar ratio suggested that the Cu^{2+} adsorption into the STPP crosslinked chitosan might be related to 2 adsorption mechanisms, i.e. the ionic adsorption due to interaction between phosphate functional group (PO_4^{3-}) of STPP and Cu^{2+} ions and the physical adsorption in the network structure of crosslinked chitosan. When using low Cu^{2+} initial concentration, the ionic adsorption was considered to be the main mechanism of Cu^{2+} uptake into the

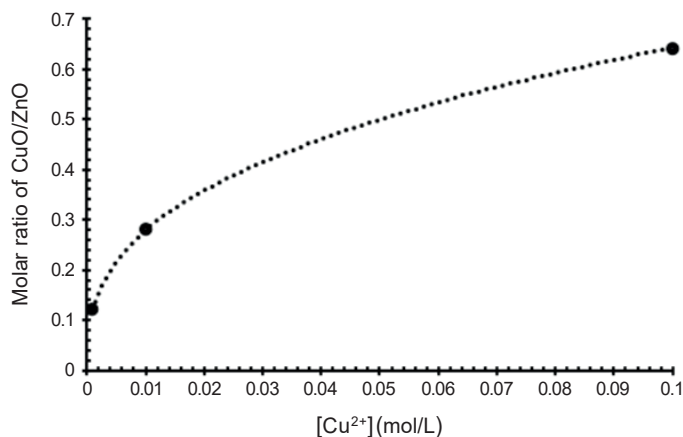


Fig. 1. Quantity of Cu²⁺ uptake in the chitosan/Cu²⁺ precursors represented in the form of CuO/ZnO molar ratio as a function of initial Cu²⁺ concentration

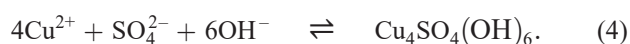
crosslinked chitosan, resulting in the steep increase of CuO/ZnO molar ratio. If the high Cu²⁺ initial concentration was used, the surplus Cu²⁺ uptake was mainly due to the physical adsorption.

3.2. Characterization of chitosan/CuO nanocomposites.

Figure 2 shows the XRD patterns and SEM micrographs of the chitosan/CuO nanocomposites obtained from hydrothermal treatment in the NaOH media. The XRD patterns of all Chi/CuO-Na nanocomposites showed two main crystalline peaks at 2θ = 36.63° and 42.55° superimposed on the broad amorphous signal, in which these crystalline peaks corresponded to CuO (PDF No. 78–0428). These results indicated the hydrothermal growth of CuO in the crosslinked chitosan matrix due to the reaction between the adsorbed Cu²⁺ in the precursors and the OH⁻ in the basic media as shown in the chemical equation (2) and (3):



In Fig. 2(a), the XRD pattern of Chi/0.001CuO-Na sample showed the poorly crystalline CuO was obtained. The formation of high crystallinity of CuO can be clearly observed in the XRD patterns of Chi/0.01CuO-Na and Chi/0.1CuO-Na samples as respectively shown in Fig.2(b) and Fig.2(c), suggesting that the well-crystallized CuO was obtained in both conditions. However, the crystalline peaks of Cu₄SO₄(OH)₆ (PDF No. 43–1458) were also clearly observed in the Chi/0.1CuO-Na sample, in which it might be because the excessive amount of CuSO₄ was physically adsorbed in the Chi/0.1Cu²⁺ precursor could react with the OH⁻ in the basic media as shown in the chemical equation (4):



The crystallite size attributed to the *111*-plane (2θ = 36.63°) of hydrothermally grown CuO in the NaOH media increased with the increase of Cu²⁺ initial concentration used in the preparation of chitosan/Cu²⁺ precursors as shown in Table 2.

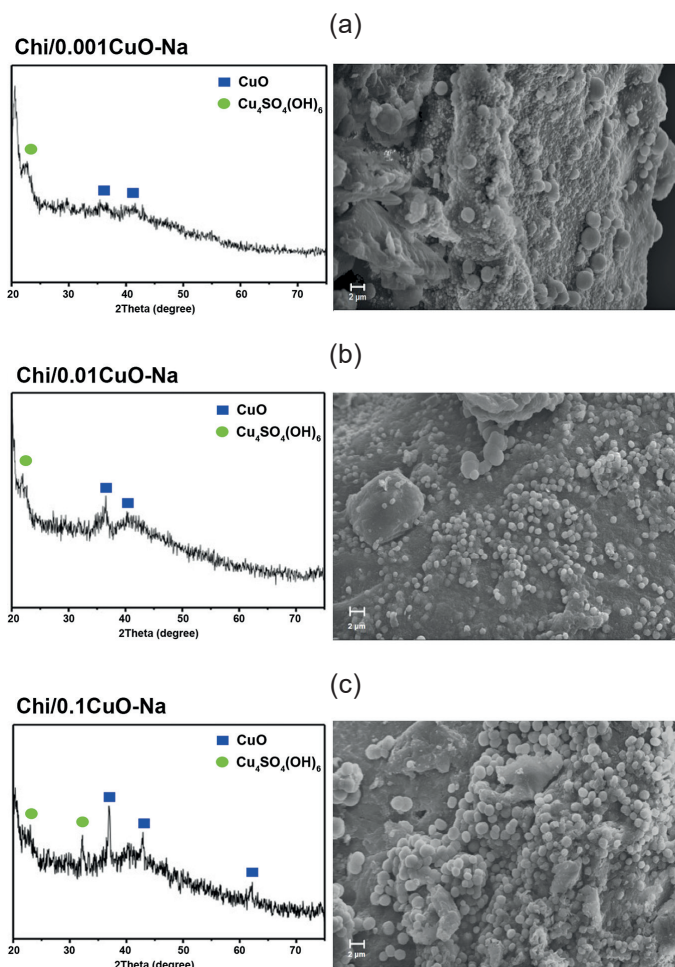


Fig. 2. XRD patterns and SEM micrographs of the chitosan/CuO nanocomposites obtained from hydrothermal treatment in the NaOH media: (a) Chi/0.001CuO-Na, (b) Chi/0.01CuO-Na and (c) Chi/0.1CuO-Na

Table 2

Crystallite size of CuO hydrothermally grown in the chitosan/CuO nanocomposites and zone of inhibition (in mm) of chitosan/CuO nanocomposites against bacterial strains

Sample	Initial concentration of CuSO ₄ ·5H ₂ O (mol/L)	Hydrothermal media	Crystallite size* (nm)	Diameter of inhibition zone (mm)	
				<i>S. aureus</i>	<i>E. coli</i>
Chi/0.001CuO-Na	0.001	NaOH	39.34	0	0
Chi/0.01CuO-Na	0.01	NaOH	41.84	9.5	8
Chi/0.1CuO-Na	0.1	NaOH	74.67	10	9
Chi/0.001CuO-NH	0.001	NH ₄ OH	17.58	0	0
Chi/0.01CuO-NH	0.01	NH ₄ OH	30.76	9	8
Chi/0.1CuO-NH	0.1	NH ₄ OH	41.02	9.5	9

*Calculated from Scherrer's equation using FWHM of the crystalline peak at 2θ = 36.63°

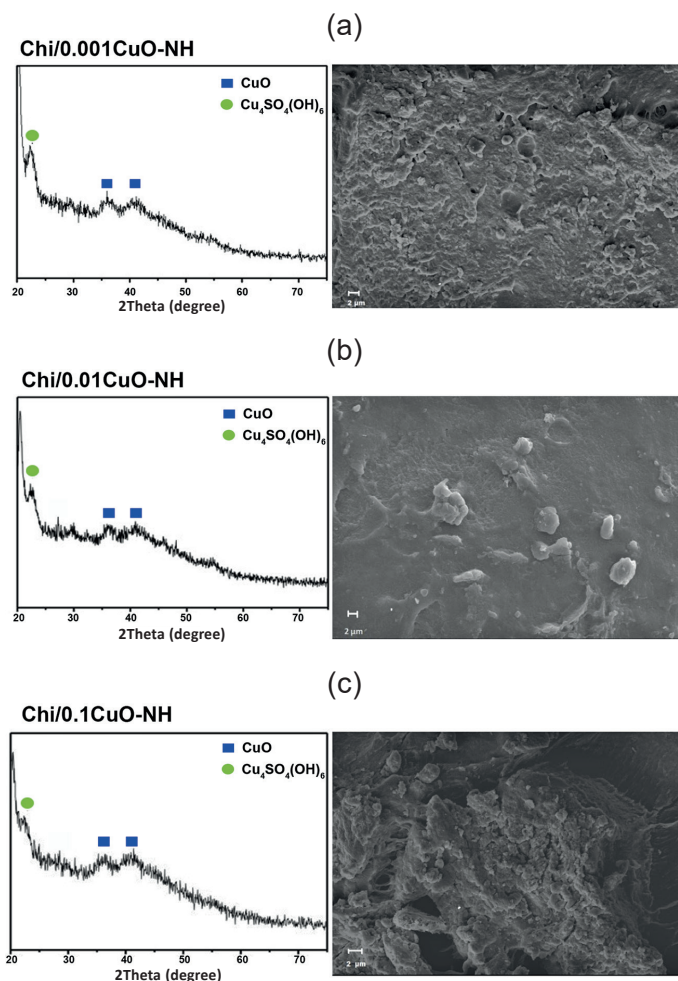


Fig. 3. XRD patterns and SEM micrographs of the chitosan/CuO nanocomposites obtained from hydrothermal treatment in the NH_4OH media: (a) Chi/0.001CuO-NH, (b) Chi/0.01CuO-NH and (c) Chi/0.1CuO-NH

The CuO crystals were observed in the SEM micrographs as well-dispersed uniform spherical particles, in which these particles partially embedded in the continuous phase of chitosan matrix. However, the formation of agglomerated CuO particles was also observed on the surface of Chi/0.1CuO-Na sample having the highest CuO content as shown in Fig. 2(c).

Figure 3 shows the XRD patterns and SEM micrographs of the chitosan/CuO nanocomposites obtained from hydrothermal treatment in the NH_4OH media. The crystalline peaks of CuO at $2\theta = 36.63^\circ$ and 42.55° were observed in all XRD patterns, in which they were superimposed on the broad amorphous signal of chitosan matrix. The hydrothermal growth of CuO in the NH_4OH media occurred through the chemical reactions shown in equation (2) and (3). From Table 2, the smaller crystallite size of CuO obtained in all Chi/CuO-NH nanocomposites exhibited the broader CuO peaks than those in the Chi/CuO-Na nanocomposites. These results were considered to be because the NaOH is a strong base which completely dissociates in water; therefore, it can promote the growth of CuO. The higher Cu^{2+} initial concentration used in the precursor preparation, the larger CuO crystallite size was obtained in the Chi/CuO-NH nanocomposites. The SEM micrographs of Chi/CuO-NH nanocomposites were observed as rough surfaces; however, the formed CuO crystals could not be clearly seen. These results might be because the CuO crystals grew in the NH_4OH media were mostly embedded in the crosslinked chitosan matrix.

Figure 4 shows the schematic diagram representing the formation of network structure of crosslinked chitosan *via* the ionic bonding between the protonated chitosan (NH_3^+) and phosphate functional group (PO_4^{3-}) of STPP crosslinking agent. When the crosslinked chitosan was soaked in the $\text{CuSO}_4 \cdot 5\text{H}_2\text{O}$ solution, the Cu^{2+} cations were ionically and/or physically adsorbed into the chitosan network. The crosslinked chitosan network acted as the host template for hydrothermal growth of CuO nanocrystals in the basic solutions.

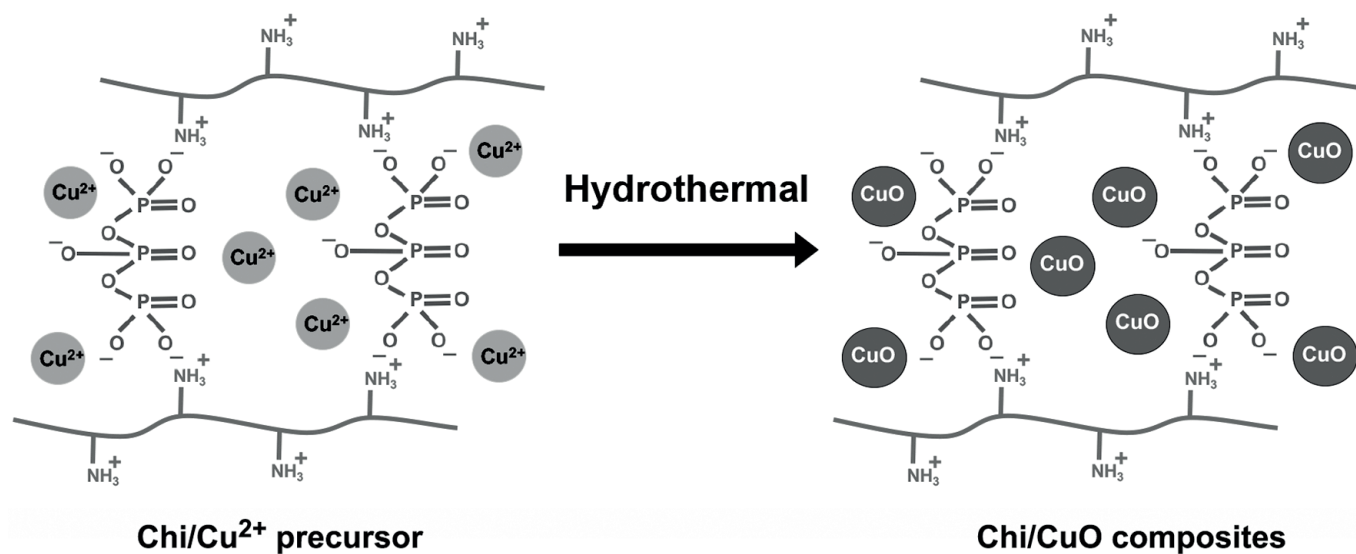


Fig. 4. Schematic illustration of the formation of network structure of crosslinked chitosan

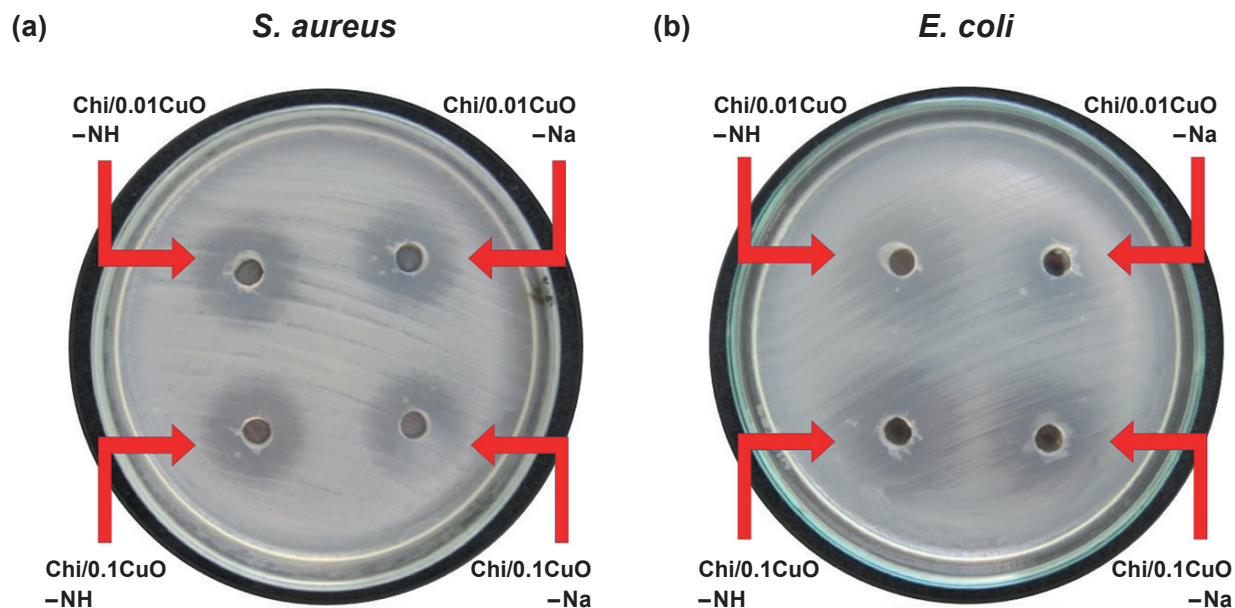


Fig. 5. Antibacterial activities of chitosan/CuO nanocomposites against the gram positive *S. aureus* (a) and gram negative *E. coli* (b)

3.3. Antibacterial activity of chitosan/CuO nanocomposites.

Figures 5(a) and 5(b) show the antibacterial activity of chitosan/CuO nanocomposites against the gram positive *S. aureus* and gram negative *E. coli*, respectively. It was found that the *S. aureus* and *E. coli* bacteria could grow under the Chi/0.001CuO-Na and Chi/0.001CuO-NH nanocomposites because they possessed quite low content of CuO. While, the Chi/0.01CuO-Na, Chi/0.1CuO-Na, Chi/0.01CuO-NH and Chi/0.1CuO-NH nanocomposites could inhibit the growths of *S. aureus* and *E. coli*, in which it can be clearly seen the inhibition zones as shown in Fig. 5. The diameter of inhibition zones was measured and reported in Table 2. The higher Cu²⁺ initial concentration used in the precursor preparation, the larger inhibition zone was obtained. In addition, the antibacterial activities of chitosan/CuO nanocomposites against the *S. aureus* were higher than those against the *E. coli*. The antibacterial activities of chitosan/CuO nanocomposites were attributed to the presence of CuO nanocrystals, in which the Cu²⁺ ions could be released and diffused in the agar medium. The Cu²⁺ ions could generate the reactive oxygen species (ROS) such as HO[•], O₂^{•-}, HO₂[•] and H₂O₂, then the ROS further interacted with the bacteria cells, resulting in cell integrity [17]. These results suggested that the potential use of chitosan/CuO nanocomposites synthesized by using 0.01 and 0.1 mol/L Cu²⁺ initial concentration as biocontrol agents.

4. Conclusion

The CuO nanocrystals were successfully synthesized in the ionically crosslinked chitosan network structure using facile eco-friendly hydrothermal reaction, in which the crosslinked chitosan network acted as the host template for growth of CuO

nanocrystals. The higher initial concentration of Cu²⁺ starting agent, the higher Cu²⁺ uptake was obtained in the chitosan network, resulting in the larger crystallite size of CuO nanocrystals. In addition, the crystallite size of CuO synthesized in the strong base NaOH was higher than that in the NH₄OH. These chitosan/CuO nanocomposites showed antibacterial activity preventing the growth of *S. aureus* and *E. coli*.

REFERENCES

- [1] R.J. Cava, "Structural chemistry and the local charge picture of copper oxide superconductors", *Science*, 247(4943), 656–662 (1990).
- [2] N.L. Van, C. Ma, J. Shang, Y. Rui, S. Liu, and B. Xing, "Effects of CuO nanoparticles on insecticidal activity and phytotoxicity in conventional and transgenic cotton", *Chemosphere*, 144, 661–670 (2016).
- [3] Q. Zhang, K. Zhang, D. Xu, G. Yang, H. Huang, F. Nie, C. Liu, and S. Yang, "CuO nanostructures: Synthesis, characterization, growth mechanisms, fundamental properties, and applications", *Prog. Mater. Sci.*, 60, 208–337 (2014).
- [4] G. Ren, D. Hu, E.W.C. Cheng, M.A. Vargas-Reus, P. Reip, and R.P. Allaker, "Characterisation of copper oxide nanoparticles for antimicrobial applications", *Int. J. Antimicrob. Ag.*, 33, 587–590 (2009).
- [5] S. Nations, M. Long, M. Wages, and J.D. Maul, "Subchronic and chronic developmental effects of copper oxide (CuO) nanoparticles on *Xenopus laevis*", *Chemosphere*, 135, 166–174 (2015).
- [6] J.F. Xu, W. Ji, Z.X. Shen, S.H. Tang, X.R. Ye, D.Z. Jia and X.Q. Xin, "Preparation and characterization of CuO nanocrystals", *J. Solid. State. Chem.*, 147, 516–519 (1999).
- [7] K. Chen and D. Xue, "A chemical reaction controlled mechanochemical route to construction of CuO nanoribbons for high performance lithium-ion batteries", *Phys. Chem. Chem. Phys.*, 15, 19708–19714 (2013).

- [8] S.J. Davarpanah, R. Karimian, V. Goodarzi, and F. Piri, "Synthesis of copper (II) oxide (CuO) nanoparticles and its application as gas sensor", *J. Appl. Biotechnol. Rep.*, 2, 329–332 (2015).
- [9] C. Yang, F. Xiao, J. Wang, and X. Su, "Synthesis and microwave modification of CuO nanoparticles: Crystallinity and morphological variations, catalysis, and gas sensing", *J. Colloid. Interface. Sci.*, 435, 34–42 (2014)
- [10] N.N. Mahmoud, J. Asim, and S. Numan, "Microwave synthesis of ultrathin, non-agglomerated CuO nanosheets and their evaluation as nanofillers for polymer nanocomposites", *J. Alloy. Compd.* 680, 350–358 (2016).
- [11] D. Han, H. Yang, C. Zhu and F. Wang, "Controlled synthesis of CuO nanoparticles using TritonX-100-based water-in-oil reverse micelles", *Powder. Technol.* 185, 286–290 (2008).
- [12] M. Zhang, X. Xu and M. Zhang, "Hydrothermal synthesis of sheaf-like CuO via ionic liquids", *Mater. Lett.*, 62, 385–388 (2008).
- [13] J.G. Zhao, S.J. Liu, S.H. Yang, and S.G. Yang, "Hydrothermal synthesis and ferromagnetism of CuO nanosheets", *Appl. Surf. Sci.*, 257, 9678–9681 (2011).
- [14] E.I. Rabea, M.E.T. Badawy, C.V. Stevens, G. Smagghe, and W. Steurbaut, "Chitosan as antimicrobial agent: applications and mode of action", *Biomacromolecules*, 4, 1457–1465 (2003).
- [15] J. Berger, M. Reist, J.M. Mayer, O. Felt, N.A. Peppas, and R. Gurny, "Structure and interactions in covalently and ionically crosslinked chitosan hydrogels for biomedical applications", *Eur. J. Pharm. Biopharm.* 57, 19–34 (2004).
- [16] R. Jayakumar, D. Menon, K. Manzoor, S.V. Nair, and H. Tamura, "Biomedical applications of chitin and chitosan based nanomaterials – a short review", *Carbohydr. Polym.*, 82, 227–232 (2010).
- [17] M.S. Hassan, T. Amna, O-B Yang, M.H. El-Newehy, S.S. Al-Deyab, and M-S Khil, "Smart copper oxide nanocrystals: Synthesis, characterization, electrochemical and potent antibacterial activity", *Colloids. Surf. B.*, 97, 201–206 (2012).